

APPLICATION OF A FULLY EQUILIBRATED SUPERCONVERGENT PATCH RECOVERY SCHEME FOR ERROR BOUNDING

E. Nadal*, J.P. Moitinho de Almeida[†], J.J. Ródenas*, F.J. Fuenmayor*, O.A. González-Estrada^{††}

*Centro de Investigación en Tecnología de Vehículos (CITV)
Universitat Politècnica de València, C/ Vera, s/n, E-46022-Valencia, Spain
e-mail: {jjrodena, ffuenmay}@mcm.upv.es ennasos@upvnet.upv.es

[†]Department of Civil Engineering and Architecture
Instituto Superior Técnico, Technical University of Lisbon, Lisbon, Portugal
e-mail: moitinho@civil.ist.utl.pt

^{††}Institute of Mechanics & Advanced Materials,
Cardiff University, School of Engineering, Queen's Building, The Parade, Cardiff CF24 3AA
Wales, UK.
e-mail: estradaoag@cardiff.ac.uk

Key words: Error bounding, Error estimator, Recovery technique, Statically admissible

Abstract. In this communication we present preliminary results assessing the application of a novel recovery technique, based on the well-known Superconvergent Patch Recovery (SPR) technique, to linear elasticity problems solved within the framework of the Finite Element Method (FEM). This recovery procedure provides statically admissible stress fields which are used to obtain upper bounds of the error in the energy norm. Traditionally, most error bounding approaches are residual-based, however their accuracy is not always high. Therefore practitioners and engineers generally prefer to use recovery-based techniques, because of their high accuracy and easy implementation.

Exploiting the fact that the strain energy of the difference between a kinematically admissible stress field (typically a raw FE solution) and a statically admissible stress field (for example our recovered solution) directly provides an upper bound of the error in the energy norm [1], previous recovery techniques, such as the SPR-C [2], tried to obtain upper bounds [3], relying on some correction terms, which depend on the exact solution, to account for their lack of equilibrium. In this work we compare the performance of both techniques.

1 Introduction

Numerical methods to solve Boundary Value Problems (BVP) such as the 2D linear elasticity problems have experimented a huge increase in their use by practitioners. More specifically, the displacement-based Finite Element Method (FEM) is widely used today in industries such as aerospace, civil engineering, automotive, etc. FEM is a powerful method for a vast type of engineering problems, however it is only able to provide an approximated solution. Therefore, some *error* level has to be accounted for to define the safety factors during the design process of mechanical parts.

During a Finite Element (FE) analysis there are several sources of error like geometrical simplifications of the actual component to make it suitable for the analysis, geometrical errors due to the FE discretization of the domain, the discretization error due to the FE approximation to the solution, etc. In this work we are going to focus only on the discretization error.

During the last part of the 20th century, scientist have developed techniques to obtain an estimation or a bound of the error in energy norm to quantify the quality of the FE results. The first approaches yielding upper bounds in the error estimation were based on explicit residuals [4], however their applicability is limited, since they are constant dependent. Later, a new procedure based on implicit residuals appeared which, under certain circumstances, is also able to provide upper bounds [5, 6, 7, 8, 9, 10, 11, 12]. Different approaches, related to the concept of dual analysis, working with a compatible and with an equilibrated solution, were also used to directly obtain upper error bounds. Some of them solving two global problems in parallel [13] or post-processing the FE solution [6, 14, 15]. The main characteristic of these error bounding techniques is that the error is evaluated by comparing the two solutions, one compatible and the other equilibrated, which are complementary in nature, and whose errors are orthogonal.

Other techniques, which traditionally were unable to obtain bounds for the error in energy norm, use the so-called Zienkiewicz and Zhu (ZZ) error estimator [16]. In this case the FE solution (compatible) is compared with an improved solution, not necessary equilibrated, obtained with a recovery procedure such as, e.g., the Superconvergent Patch Recovery (SPR) [17, 18]. Today, the ZZ error estimator is widely used due to its simplicity (only uses standard FE results) and high accuracy. However, the main drawback is that despite of the fact that the ZZ error estimator in combination with the SPR technique is asymptotically exact, it is unable to guarantee an upper bound of the error in energy norm.

Some works to improve the original SPR technique have been carried out. Ródenas and *et al.* proposed to add some constraints to impose local equilibrium to the recovered solution [2] obtaining a quasi-equilibrated recovered solution, using the so-called SPR-C technique. Díez *et al.*[3] presented a methodology to obtain computable upper bounds of the error in energy norm considering the quasi-equilibrated recovered field. Those ideas were also applied by Ródenas and co-workers [19, 20, 21, 22] in the eXtended Finite

Element Method (XFEM) framework [23, 24]. In all those methods the upper bound property was not strongly guaranteed by using directly the recovered solution. Thus, they needed the evaluation of some correction terms to compute the lack of equilibrium [3] for which only an estimation was available.

In this work, we present a procedure which directly recovers a fully equilibrated recovered solution from the superconvergent stresses. Then, directly comparing the FE solution with the recovered one, using a version of the ZZ error estimator, we obtain guaranteed upper bounds of the error in the energy norm, yielding sharp estimations as shown in the section devoted to numerical tests.

2 Problem Statement

Let us consider the displacement field \mathbf{u} taking values in $\Omega \subset \mathbb{R}^2$ as the solution of the 2D linear elasticity problem given by

$$-\nabla \cdot \boldsymbol{\sigma}(\mathbf{u}) = \mathbf{b} \quad \text{in } \Omega \quad (1)$$

$$\boldsymbol{\sigma}(\mathbf{u}) \cdot \mathbf{n} = \mathbf{t} \quad \text{on } \Gamma_N \quad (2)$$

$$\mathbf{u} = \mathbf{0} \quad \text{on } \Gamma_D \quad (3)$$

where Γ_N and Γ_D are the parts of the boundary where the Neumann and Dirichlet conditions are applied, such that $\partial\Omega = \bar{\Gamma}_N \cup \bar{\Gamma}_D$ and $\Gamma_N \cap \Gamma_D = \emptyset$. \mathbf{b} are the body loads and \mathbf{t} are the tractions imposed along Γ_N . We consider a homogeneous Dirichlet boundary condition in (3) for simplicity.

The problem can be rewritten in its variational form as:

$$\text{Find } \mathbf{u} \in V : \forall \mathbf{v} \in V \quad a(\mathbf{u}, \mathbf{v}) = l(\mathbf{v}) \quad (4)$$

where $V = \{\mathbf{v} \mid \mathbf{v} \in H^1(\Omega), \mathbf{v}|_{\Gamma_D}(\mathbf{x}) = \mathbf{0}\}$ is the standard test space for the elasticity problem. The symmetric and bilinear form $a : V \times V \rightarrow \mathbb{R}$ and the continuous linear form $l : V \rightarrow \mathbb{R}$ are defined in vectorial form as:

$$a(\mathbf{u}, \mathbf{v}) := \int_{\Omega} \boldsymbol{\sigma}^T(\mathbf{u}) \boldsymbol{\varepsilon}(\mathbf{v}) d\Omega = \int_{\Omega} \boldsymbol{\sigma}(\mathbf{u})^T \mathbf{D}^{-1} \boldsymbol{\sigma}(\mathbf{v}) d\Omega \quad (5)$$

$$l(\mathbf{v}) := \int_{\Omega} \mathbf{b}^T \mathbf{v} d\Omega + \int_{\Gamma_N} \mathbf{t}^T \mathbf{v} d\Gamma, \quad (6)$$

where $\boldsymbol{\sigma}$ represents the stresses, $\boldsymbol{\varepsilon}$ are the strains and \mathbf{D} is the elasticity matrix of the constitutive relation $\boldsymbol{\sigma} = \mathbf{D}\boldsymbol{\varepsilon}$.

3 Fully equilibrated recovery procedure

Traditionally, recovery-type error estimators were unable to provide error bounds in energy norm. Díez *et al.*[3] made a first attempt by adding some correction terms to the ZZ error estimator in order to ensure the upper bound property. In this section we are

going to show a scheme for a new recovery procedure that, directly using the ZZ error estimator, yields upper error bounds in energy norm.

When the recovered stress field $\boldsymbol{\sigma}^*$ is statically admissible in the ZZ error estimator, it yields an upper error bound. Thus, in this section we aim to the evaluation of an statically admissible stress field. To do that, $\boldsymbol{\sigma}^*$ has to fulfil the internal equilibrium equation (IEE), the boundary equilibrium equation (BE) and equilibrium of tractions along the internal element edges (IB). Note that the normal stress tangent to the boundary is no necessarily continuous along the element edges.

The technique presented here, called SPR-FE (Fully Equilibrated), is based in the SPR technique developed by Zienkiewicz and Zhu [17]. In the SPR-FE, as in SPR, we create patches of elements with the elements connected by the vertex nodes, so-called patch assembly nodes (AN), see Figure 1a. There are two main differences between the traditional SPR and the SPR-FE: a) in the SPR each recovered stress component is represented by a single polynomial on each patch, while for the SPR-FE a polynomial surface is fitted for each stress component on each element of the patch. In Figure 1a we fit, by minimizing (7), a different polynomial surface for each stress component at elements I, II, III, IV . b) the second difference is that the SPR technique builds up the global recovered field in an element by adding the contributions of each patch using a partition of unity. However, in the SPR-FE the global recovered field is obtained by directly adding the contributions of all patches $\boldsymbol{\sigma}^* = \sum_i^{AN} \boldsymbol{\sigma}_i^k$ connected to one element k since the partition of unity is implicit in the functional (7). Note that when we apply the constraints for internal and boundary equilibrium the problem loads will be also affected by the partition of unity N_i^k .

For the statically admissibility condition, we add the constraints that are necessary to enforce the required continuity and equilibrium in the recovered solution using a point collocation approach, the number of points will depend on the degree of the recovered field. This is obtained by adding continuity of tractions along the internal edges (red edges). We enforce the recovered tractions to zero along the external edges (blue edges) and finally we enforce the equilibrium equation at each element, separately. The recovery process will be described below in more detail.

3.1 Recovery procedure

We minimize the following functional on each of the k elements of the patch with assembly node i :

$$\Psi = \int_{\Omega_k} (\boldsymbol{\sigma}_k^* - N_i^k \boldsymbol{\sigma}^h)^2 d\Omega \quad k = I, II, III, IV \quad (7)$$

where N_i^k is the linear shape function of the node i , in element k . $\boldsymbol{\sigma}^h$ is the FE stress field and $\boldsymbol{\sigma}_k^* = \mathbf{P}_k \mathbf{a}_k$ is the recovered stress field for the element k , where $\mathbf{a}_k = \{\mathbf{a}_k^{xx}, \mathbf{a}_k^{yy}, \mathbf{a}_k^{xy}\}^T$ are the coefficients for each stress component and \mathbf{P}_k is the matrix for the polynomial expansion $\mathbf{p}_k = \{x^m y^n : m, n \leq q\}_k$, where q is the polynomial degree

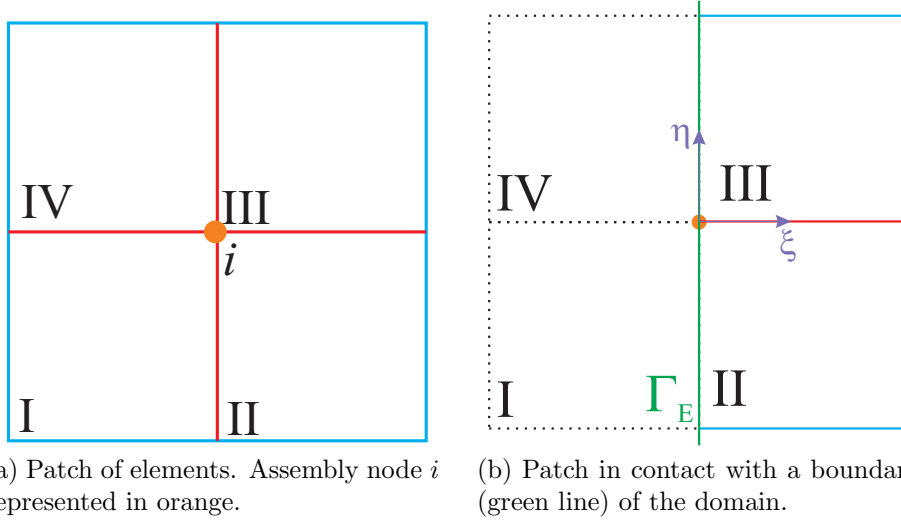


Figure 1: Internal patch formed by 4 elements (left) and patch in contact with the boundary formed by 2 elements (right).

$$\mathbf{P}_k = \begin{bmatrix} \mathbf{p}_k & 0 & 0 \\ 0 & \mathbf{p}_k & 0 \\ 0 & 0 & \mathbf{p}_k \end{bmatrix} \quad (8)$$

For each element k , integrating numerically after the minimization of (7) we obtain the following expression:

$$\sum_{pg} \mathbf{P}_k^T \mathbf{P}_k |\mathbf{J}| \omega \mathbf{a}_k = \sum_{pg} \mathbf{P}_k^T N_i^k \boldsymbol{\sigma}^h |\mathbf{J}| \omega \quad (9)$$

where $|\mathbf{J}|$ is the Jacobian of the coordinates transformation, ω is the weight of each integration point and pg is the number of integration points. This expression yields a linear system of equations for each element of the patch $\mathbf{M}_k \mathbf{a}_k = \mathbf{g}_k$. Due to the constraints we have imposed, we need some interaction between the different recovered stress fields. Thus, we assemble all four systems together and we obtain the following linear system for the patch:

$$\begin{bmatrix} \mathbf{M}_I & 0 & 0 & 0 \\ 0 & \mathbf{M}_{II} & 0 & 0 \\ 0 & 0 & \mathbf{M}_{III} & 0 \\ 0 & 0 & 0 & \mathbf{M}_{IV} \end{bmatrix} \begin{Bmatrix} \mathbf{a}_I \\ \mathbf{a}_{II} \\ \mathbf{a}_{III} \\ \mathbf{a}_{IV} \end{Bmatrix} = \begin{Bmatrix} \mathbf{g}_I \\ \mathbf{g}_{II} \\ \mathbf{g}_{III} \\ \mathbf{g}_{IV} \end{Bmatrix} \Rightarrow \mathbf{M} \mathbf{a} = \mathbf{g} \quad (10)$$

3.2 Internal equilibrium constraint

In contrast with the SPR-C presented in [2], where the internal equilibrium equation was $\nabla \cdot \boldsymbol{\sigma}_k^* + \mathbf{b} = 0$, in the SPR-FE we have to take into account the partition of unity

introduced in the functional (7). Therefore, it will affect to the body forces \mathbf{b} and also bring up a new term, first introduced in [15]: *the fictitious body forces*, $\nabla N_i^k \boldsymbol{\sigma}^h$. Their role is to ensure that the forces applied to each patch satisfy global equilibrium for the isolated patch. If their were not considered, then Equation (10), would generally have no solution. Nevertheless, when we sum up the contributions of the four patches of a single element k these terms will sum to zero, cancelling their effect at a global level.

Then, the internal equilibrium equation to impose in this case is $\nabla \cdot \boldsymbol{\sigma}_k^* + N_i^k \mathbf{b} = \nabla N_i^k \boldsymbol{\sigma}^h$ at each element k . These constraints are independently enforced in all elements. This generates the internal equilibrium matrix for each element \mathbf{C}_k^{IEE} and the independent term \mathbf{h}_k^{IEE} .

3.3 External patch edge constraint

The next step is to add the constraints along the external boundaries of the patch, that is, the constraints along the blue edges in Figure 1a. These constraints will ensure tractions continuity when we sum up the contributions from the patches related to an element. Since the partition of unity function is zero at the external edges of the patch, the equation to be imposed there is $\boldsymbol{\sigma}_k^* \cdot \mathbf{n} = \mathbf{0}$, where \mathbf{n} is the outward normal vector along the patch boundary. This generates for each element the matrix \mathbf{C}_k^{BE} and the independent term $\mathbf{h}_k^{BE} = \mathbf{0}$.

3.4 Internal patch edge constraint

Finally, it is also necessary to add the constraints along the internal boundaries of the patch (red edges), *i.e.* the interfaces between elements. These are also used to ensure tractions continuity along the element interface. The equation to be imposed is $\boldsymbol{\sigma}_k^* \cdot \mathbf{n}_k + \boldsymbol{\sigma}_l^* \cdot \mathbf{n}_l = \mathbf{0}$, where $k \neq l$, \mathbf{n}_k and \mathbf{n}_l are the outward normal vectors of each elements in the common edge ($\mathbf{n}_k = -\mathbf{n}_l$), generating \mathbf{C}_k^{IB} and \mathbf{C}_l^{IB} respectively, the RHS is again null $\mathbf{h}_k^{IB} = \mathbf{0}$.

A particular situation occurs when an internal edge coincides with a boundary where the tractions are prescribed. In Figure 1b we illustrate such a boundary (green line), which is internal to the patch. This is a typical situation when the assembly nodes (orange point) are over the boundary. In this case, the equations to be imposed have to take into account the Neumann boundary condition then, $\boldsymbol{\sigma}_k^* \cdot \mathbf{n}_k = N_i^k \mathbf{t}$. When the boundary condition is non-homogeneous the corresponding term in the RHS is generally not null, $\mathbf{h}_k^{IB} \neq \mathbf{0}$. Note that the opposite element sharing the edge, *i.e.* element l in the general case, does not exist for this type of patch.

3.5 System resolution considerations

Adding all constraints to (10) we obtain the following linear system to solve at each patch:

$$\begin{bmatrix} \mathbf{M} & (\mathbf{C}^{IEE})^T & (\mathbf{C}^{EB})^T & (\mathbf{C}^{IB})^T \\ \mathbf{C}^{IEE} & 0 & 0 & 0 \\ \mathbf{C}^{EB} & 0 & 0 & 0 \\ \mathbf{C}^{IB} & 0 & 0 & 0 \end{bmatrix} \begin{Bmatrix} \mathbf{a} \\ \lambda^{IEE} \\ \lambda^{EB} \\ \lambda^{IB} \end{Bmatrix} = \begin{Bmatrix} \mathbf{g} \\ \mathbf{h}^{IEE} \\ 0 \\ \mathbf{h}_k^{IB} \end{Bmatrix} \quad (11)$$

and it could be rewritten as $\mathbf{M}_C \mathbf{a}_C = \mathbf{g}_C$, where C indicates that the constraints are included.

The basis \mathbf{p} for the stress field has to be able to represent all constraints to guarantee the statical admissibility property. Thus, we need to analyse the minimum degree required for the stress field to guarantee the equations system (11) is solvable. We consider a bi-quadratic representation of the displacement field. Linear or bilinear FE solutions cannot be directly applied to this recovery procedure since they do not guarantee rotational equilibrium of the patch [25]. Then, the FE stress field $\boldsymbol{\sigma}^h$ has quadratic terms, the partition of unity used in (7) is bilinear and its divergence has linear terms. Analyzing the constraints we need at least a 4th order polynomial interpolation because of the fictitious body forces. In Table 1 we show the total size of the system to be solve at each node. We have to pay attention to the “effective” number of “free coefficients” (last column), the difference between the number of “Coefficients” \mathbf{a} and the number of independent constraints. For degree 4 there are more constraints (192+80+40 = 300) than coefficients, therefore some constraints have to be linearly dependent. In fact there are always linearly dependent constraints, as indicated by the difference between the dimension of the system and its rank, and thus we obtain 16 effective free coefficients for degree 4. We use the Singular Value Decomposition (SVD) technique to solve that system, identifying the dependent equations and their consistency.

Degree	Coefficients	IEE ctr	EB ctr	IB ctr	System size	Rank	Eff free coef
4	300	192	80	40	612	584	16
5	432	280	96	48	856	828	40
6	588	384	112	56	1140	1108	68

Table 1: Number of coefficients and constraints

4 Numerical results

In this section we verify numerically that the upper bound property is satisfied by the error estimation when the SPR-FE is used in the ZZ error estimator in (12). We also define the global effectivity index $\theta = \|\mathbf{e}_{es}\|/\|\mathbf{e}\|$ as the ratio between the estimated error $\|\mathbf{e}_{es}\|$ and the exact error, where $\boldsymbol{\sigma}$ is the exact stress field:

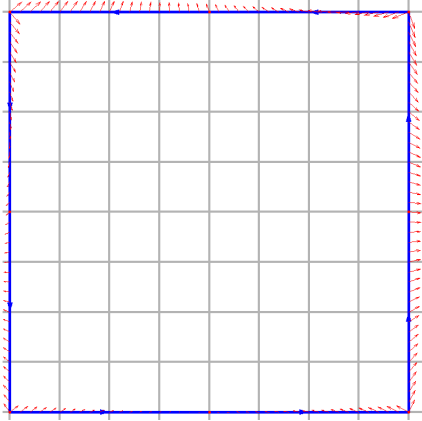
$$\|\mathbf{e}_{es}\|^2 = \int_{\Omega} (\boldsymbol{\sigma}^* - \boldsymbol{\sigma}^h)^T \mathbf{D}^{-1} (\boldsymbol{\sigma}^* - \boldsymbol{\sigma}^h) d\Omega \quad (12)$$

$$\|\mathbf{e}\|^2 = \int_{\Omega} (\boldsymbol{\sigma} - \boldsymbol{\sigma}^h)^T \mathbf{D}^{-1} (\boldsymbol{\sigma} - \boldsymbol{\sigma}^h) d\Omega \quad (13)$$

We compare the results obtained with the SPR-FE with those obtained with the SPR-C [2]. In all problems, plane strain and bi-quadratic elements will be considered for all analyses.

4.1 Problem 1. 2×2 square

This problem has an analytical cubic solution in displacements with body forces. The problem model, material properties and exact solution are represented in Figure 2.



$$\begin{aligned} u_x &= x + x^2 - 2xy + x^3 - 3xy^2 + x^2y \\ u_y &= -y - 2xy + y^2 - 3x^2y + y^3 - xy^2 \\ \sigma_{xx} &= \frac{E}{1+\nu} (1 + 2x - 2y + 3x^2 - 3y^2 + 2xy) \\ \sigma_{yy} &= \frac{-E}{1+\nu} (1 + 2x - 2y + 3x^2 - 3y^2 + 2xy) \\ \sigma_{xy} &= \frac{E}{1+\nu} (-x - y + \frac{x^2}{2} - \frac{y^2}{2} - 6xy) \\ b_x &= \frac{-E}{1+\nu} (1 + y) \quad b_y = \frac{-E}{1+\nu} (1 - x) \\ E &= 1000, \nu = 0.3 \end{aligned}$$

Figure 2: Problem 1. Model, material and analytical solution.

Figure 3 shows the results obtained with the SPR-FE recovered stress field with 4th (blue line) and 5th (red line) order polynomial interpolation. Black lines correspond to the results obtained with the SPR-C technique. In terms of effectivity of the error estimator, we observe that in all cases θ is above 1 (satisfies the upper bound property) and very close to 1 (very accurate error estimation). Theoretically, for the SPR-FE the upper bound is guaranteed but not for the SPR-C, however the results are quite similar. Regarding the computational cost, we observe a considerable difference between the techniques. This is due to the complexity of the technique used to solve system (11).

4.2 Problem 2. 2×2 square in cylinder under internal pressure

The analytical solution of this problem corresponds to a pipe under internal pressure. However, we have extract form the problem an squared area (green area) for the analysis and we have run the FE analysis applying the corresponding Neumann boundary conditions and constraining the rigid body motions. The problem model, material properties and exact solution is represented in Figure 4, in polar coordinates.

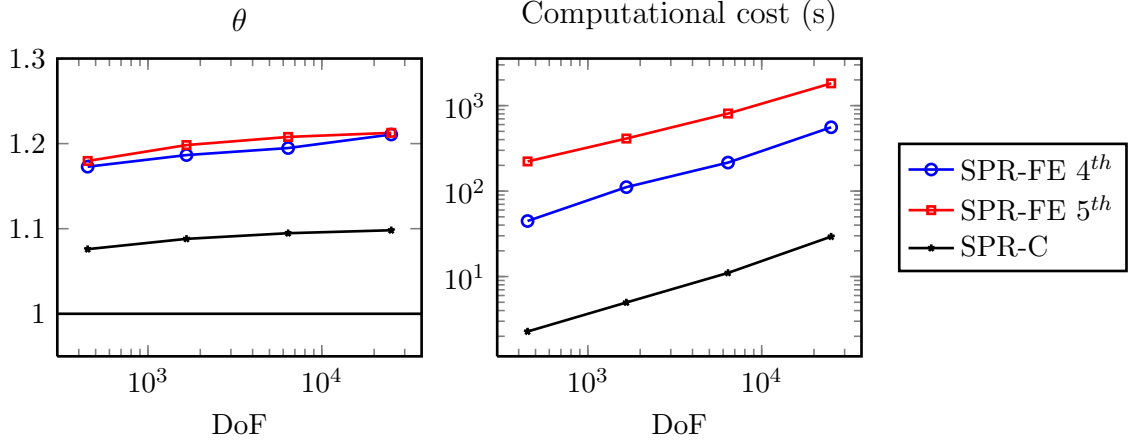
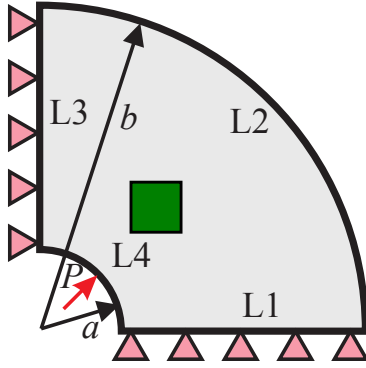


Figure 3: Problem 1. Q8. Global effectivity index θ and overall computational cost for SPR-FE and SPR-C techniques.



$$\begin{aligned}
 u_r(r) &= \frac{P(1+\nu)}{E(c^2-1)} \left(r(1-2\nu) + \frac{b^2}{r} \right) \\
 \sigma_r(r) &= \frac{P}{c^2-1} \left(1 - \frac{b^2}{r^2} \right) \\
 \sigma_\theta(r) &= \frac{P}{c^2-1} \left(1 + \frac{b^2}{r^2} \right) \\
 a &= 5 \quad b = 20 \quad P = 1 \\
 E &= 1000 \quad \nu = 0.3 \quad c = \frac{b}{a}
 \end{aligned}$$

Figure 4: Problem 2: Model, material and analytical solution.

For this problem the upper bound property is not strictly guaranteed because the tractions over the boundary of the domain (green area) cannot be represented by the polynomial basis used for the recovery. However, in Figure 5 we observe again an upper bound for the two techniques and the results are very accurate for all of them.

5 Conclusions

In this work we have presented a novel technique that is able to provide an upper error bound in energy norm. This technique is based on the ZZ error estimator and it uses an elaborated recovery procedure. Results showed that the computational cost to obtain that recovered field is quite high in comparison with standard recovery procedures. The main advantage of the SPR-FE is that, in contrast with other recovery procedures

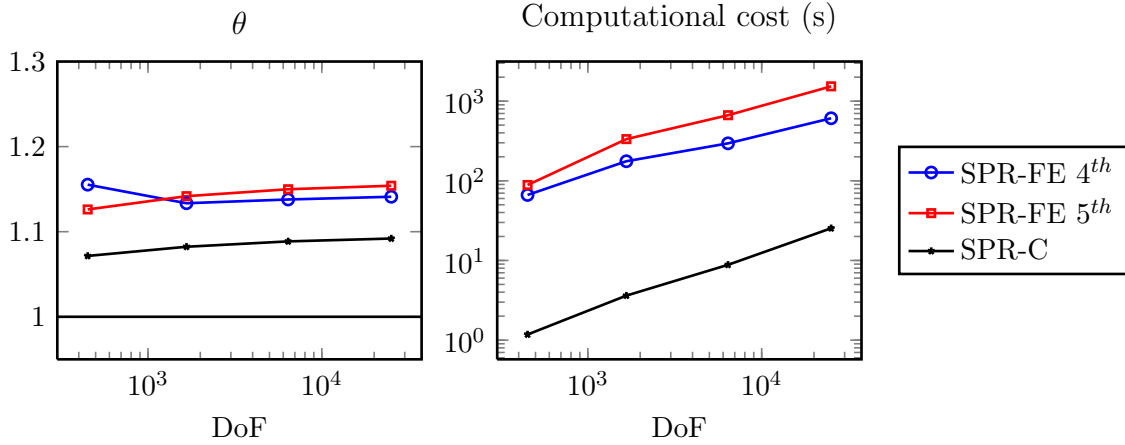


Figure 5: Problem 2. Q8. Global effectivity index θ and computational cost for SPR-FE and SPR-C techniques.

such as the SPR-C, it is able to obtain guaranteed error bounds without any correction terms. Nevertheless, the SPR-C is obtaining for these examples numerical upper bounds and error estimates close to one. We are currently working to improve the computational cost associated to the SPR-FE to make it competitive with traditional error bounding techniques.

ACKNOWLEDGEMENTS

This work has been carried out within the framework of the research project DPI2010-20542 of the Ministerio de Economía y Competitividad (Spain). The financial support of the FPU program (AP2008-01086), the funding from Universitat Politècnica de València and Generalitat Valenciana (PROMETEO/2012/023) are also acknowledged. This work was also supported by the EPSRC grant EP/G042705/1. The authors also thank the support of the Framework Programme 7 Initial Training Network Funding under grant number 289361 “Integrating Numerical Simulation and Geometric Design Technology.”

REFERENCES

- [1] Práger W, Synge JL. Approximation in elasticity based on the concept of function space. *Quart. Appl. Math.* 1947; **5**:241–269.
- [2] Ródenas JJ, Tur M, Fuenmayor FJ, Vercher A. Improvement of the superconvergent patch recovery technique by the use of constraint equations: the SPR-C technique. *International Journal for Numerical Methods in Engineering* 2007; **70**(6):705–727.
- [3] Díez P, Ródenas JJ, Zienkiewicz OC. Equilibrated patch recovery error estimates: simple and accurate upper bounds of the error. *International Journal for Numerical Methods in Engineering* 2007; **69**(10):2075–2098.

- [4] Babuška I. Error-Bounds for Finite Element Method. *Numerische Mathematik* 1970; **16**:322–333.
- [5] Babuška I, Rheinboldt WC. A-posteriori error estimates for the finite element method. *International Journal for Numerical Methods in Engineering* 1978; **12**(10):1597–1615.
- [6] Ladevèze P, Leguillon D. Error estimate procedure in the finite element method and applications. *SIAM Journal on Numerical Analysis* 1983; **20**(3):485–509.
- [7] Ladevèze P, Maunder EAW. A general method for recovering equilibrating element tractions. *Computer Methods in Applied Mechanics and Engineering* 1996; **137**(2):111–151.
- [8] Ladevèze P, Rougeot P. New advances on a posteriori error on constitutive relation in fe analysis. *Computer Methods in Applied Mechanics and Engineering* 1997; **150**(1-4):239–249.
- [9] Ladevèze P, Rougeot P, Blanchard P, Moreau JP. Local error estimators for finite element linear analysis. *Computer Methods in Applied Mechanics and Engineering* 1999; **176**(1-4):231–246.
- [10] Pled F, Chamoin L, Ladevèze P. An enhanced method with local energy minimization for the robust a posteriori construction of equilibrated stress fields in finite element analyses. *Computational Mechanics* Sep 2011; .
- [11] Díez P, Parés N, Huerta A, Díez P, Pares N. Recovering lower bounds of the error by postprocessing implicit residual a posteriori error estimates. *International Journal for Numerical Methods in Engineering* Mar 2003; **56**(10):1465–1488.
- [12] Díez P, Parés N, Huerta A. Accurate upper and lower error bounds by solving flux-free local problems in stars. *Revue européenne des éléments finis* 2004; **13**(5-6-7):497.
- [13] Pereira OJBA, de Almeida JPM, Maunder EAW. Adaptive methods for hybrid equilibrium finite element models. *Computer Methods in Applied Mechanics and Engineering* 1999; **176**(1-4):19–39.
- [14] Almeida OJB, Moitinho JP. A posteriori error estimation for equilibrium finite elements in elastostatic problems. *Computer Assisted Mechanics and Engineering Sciences* 2001; **8**(2-3):439–453.
- [15] Moitinho JP, Maunder EAW. Recovery of equilibrium on star patches using a partition of unity technique. *International journal for ...* 2009; **79**:1493–1516.

- [16] Zienkiewicz OC, Zhu JZ. A simple error estimator and adaptive procedure for practical engineering analysis. *International Journal for Numerical Methods in Engineering* 1987; **24**(2):337–357.
- [17] Zienkiewicz OC, Zhu JZ. The superconvergent patch recovery and a posteriori error estimates. Part 1: The recovery technique. *International Journal for Numerical Methods in Engineering* 1992; **33**(7):1331–1364.
- [18] Zienkiewicz OC, Zhu JZ. The superconvergent patch recovery and a posteriori error estimates. Part 2: Error estimates and adaptivity. *International Journal for Numerical Methods in Engineering* 1992; **33**(7):1365–1382.
- [19] Ródenas JJ, Giner E, Fuenmayor FJ, González-Estrada OA. Accurate recovery-type error estimation for linear elastic fracture mechanics in FEM and X-FEM based on a singular+smooth field splitting. *International Conference on Adaptive Modeling and Simulation. ADMOS 2007*, International Center for Numerical Methods in Engineering (CIMNE), 2007; 202–205.
- [20] Ródenas JJ, González-Estrada OA, Tarancón JE, Fuenmayor FJ. A recovery-type error estimator for the extended finite element method based on singular+smooth stress field splitting. *International Journal for Numerical Methods in Engineering* 2008; **76**(4):545–571.
- [21] Ródenas JJ, González-Estrada OA, Díez P, Fuenmayor FJ. Upper bounds of the error in the extended finite element method by using an equilibrated-stress patch recovery technique. *International Conference on Adaptive Modeling and Simulation. ADMOS 2007*, International Center for Numerical Methods in Engineering (CIMNE), 2007; 210–213.
- [22] Ródenas JJ, González-Estrada OA, Díez P, Fuenmayor FJ. Accurate recovery-based upper error bounds for the extended finite element framework. *Computer Methods in Applied Mechanics and Engineering* 2010; **199**(37-40):2607–2621.
- [23] Moës N, Dolbow J, Belytschko T. A finite element method for crack growth without remeshing. *International Journal for Numerical Methods in Engineering* 1999; **46**(1):131–150.
- [24] Sukumar N, Prévost JH. Modeling quasi-static crack growth with the extended finite element method. {Part I}: Computer implementation. *International Journal of Solids and Structures* 2003; **40**(26):7513–7537.
- [25] Maunder EAW, Moitinho JP. Recovery of equilibrium on star patches from conforming finite elements with a linear basis. *International Journal for ...* 2012; **89**:1497–1526.